Multilayered manufacturing method for microfluidic systems using low-cost, resin-based 3D printing

Victor Edi Manqueros Aviles *, Hesner Coto Fuentes, Karla Victoria Guevara Amaton, Francisco Valdés Perezgasga, Julián Alonso-Chamarro

Posted Date: 24 December 2024

doi: 10.20944/preprints202412.2045.v1

Keywords: Microfluidics; Resin-based 3D printing; Fabrication

Article

Multilayered manufacturing method for microfluidic systems using low-cost, resin-based 3D printing

Victor Edi Manqueros-Avilés [1,*,†], Hesner Coto-Fuentes [1,†], Karla Victoria Guevara-Amatón [1], Francisco Valdés-Perezgasga [1] and Julian Alonso-Chamarro [2]

[1] Tecnológico Nacional de México/Instituto Tecnológico de la Laguna, Cuauhtémoc y Revolución s/n, Torreón Coahuila 27000, México
[2] Group of Sensors and Biosensors, Department of Chemistry, Autonomous University of Barcelona, Edific Cn, 08193 Barcelona, Spain
* Correspondence: edi.ma@itslerdo.edu.mx
† These authors contributed equally to this work.

Abstract: The present work addresses a method, based on multilamination, for the fabrication of microfluidic devices or analytical microsystems using only commercially available 3D printers and photocurable resins. The created devices were used for the colorimetric measurement of copper ions in aqueous solutions, yielding results comparable to traditional cyclic olefin copolymer (COC) systems but with a significant cost reduction. The microfluidic platforms showed stability and functionality over a twelve-week testing period. This study highlights the potential of 3D printing as a flexible, efficient, and cost-effective alternative for the fabrication of customized microfluidic devices, promoting its use in research with limited resources.

Keywords: Microfluidics; Resin-based 3D printing; Fabrication

1. Introduction

Microfluidics is the field that studies the handling of very small amounts of fluids. It has seen an exponential growth allowing for its application in a wide variety of scientific and technological fields including biology, chemistry, medicine and engineering. The precise manipulation of fluids using small channels has produced miniaturized systems that have been applied to medical diagnostics, disease detection and chemical and biological analyses [1–3]. However, the selection of materials and fabrication techniques is a critical factor as it influences critically the efficiency, economic viability and the accessibility of these microsystems.

Early microfluidic devices were built on silicon or glass using microelectronic techniques including lithography and etching producing devices with high precision, highly miniaturization and quality but at a high cost and very strict environmental requirements such as the use of clean rooms.

Once microfluidic devices proved their worth, the development of novel applications growed very rapidly thanks to the use of new materials and simpler and cheaper microfabrication methods.

Computer controlled machining (CNC) and laser machining are currently used on polymer substrates. For instance, computer-controlled machining (CNC) and laser machining are currently used on a wide variety of polymeric substrates.

These techniques can produce microstructures in a fast and precise manner rendering them ideal to produce prototypes or small series of devices. CNC micromachining is especially useful when working with thermoplastic substrates as it is a good compromise between substrate costs, fabrication speed and surface quality. On the other hand, laser micromachining allows for an even greater precision. Both technologies call for the use of equipment whose cost ranges from medium to high.

Additionally, methods such as microembossing and microinjection continue to be essential for the mass production of microfluidic devices. These processes enable the fabrication of devices

 doi:10.20944/preprints202412.2045.v1

featuring high-quality surfaces and high reproducibility but require a much higher investment in specialized machinery to produce the required molds.

However, this approach is mainly preferred for industrial production as this higher investment is dampened by spreading it in the high yield of mass-produced devices.

Fabrication methods based on layers or multilamination have recently become popular due to their ability to build devices with complex geometries and convoluted designs as these devices cannot be produced at a reasonable cost using other methods. Multilamination involves making a 3D structure layer by layer using a single or several materials that can be different or the same.

This involves several micromachining techniques capable of defining different motifs and structures in each layer.

The ensuing 3D structure can integrate different functionalities such as microfluidic channels, electronic circuits, sensors and other detection systems. Making devices layer by layer permits the construction of devices featuring material gradients or devices with adjustable mechanical or chemical properties, a feature that may be especially valuable in biomedical and diagnostic applications.

However, these approaches require specialized thermal compression equipment like adjustable presses with hot plates that may raise the initial investment in infrastructure.

3D printing is an emergent technology in the fabrication of microfluidic devices. It involves methods such as stereolithography (SLA), fused deposition modeling (FDM), selective laser sintering (SLS) and multijet modeling (MJM), that produce complex 3D structures one layer at a time. Each of these methods has its own combination of cost, processing speed, resolution and design complexity.

For instance, SLA and SLS provide the high resolution and precision needed to produce complex microfluidic structures but at a relatively high cost.

On the other hand, FDM is a more economic option but with some limitations in resolution and surface quality [4,5].

Although 3D printing is considered a layer-by-layer additive manufacturing technology it is key to differentiate it with respect to other layer technologies such as multilamination.

In 3D printing the resulting structure is produced by the segmentation of the object in layers. Each layer is formed and fused with the previous layer in a continuous printing process.

In multilamination, layers are fabricated separately and then aligned and processed by different ways (thermo compression, sinterization, gluing, etc.) so all the layers are fused in a single and final 3D object.Low-temperature co-fired ceramics (LTCC) and cyclic olefin copolymer (COC) are two materials widely used to fabricate microfluidic devices using the multilamination approach. Both these materials and the associated technology show advantages and disadvantages depending on the application. Although development costs are much lower than the methods described above, they are still out of reach for researchers with limited research funds.

LTCC technology allows for the integration of microchannels, valves, sensing elements and signal-processing circuitry. This approach yields robust and precise microfluidic systems that have been applied to biomedical, diagnostic and chemical problems.

Although LTCC-based microfluidic systems are versatile, they require special materials with adequate thermal compatibility such as substrates, inks, pastes, etc. and costly equipment like CNC machines, presses and furnaces and this may hamper its use to obtain low-cost prototypes [6].

COC, a high-performance amorphous copolymer offers an exceptional degree of transparency and biocompatibility.

Changing the composition of the copolymer by varying the proportion of the monomers, materials with different vitreous transition temperatures can be produced.

If COC layers with different vitreous transition temperatures are used, a complex microfluidic structure can by produced in a simple manner by multilamination using a thermocompresion process.

These characteristics make COC an ideal material for applications that call for visual, optical or biological interactions [7,8]. When compared to LTCC, COC fabrication processes are simpler and

 doi:10.20944/preprints202412.2045.v1

quicker, but these processes also call for CNC machines, hot-plate precision presses or ultrasound lamination machines [9].

The present work addresses the use of photocured resins-based 3D printers combined with multilamination without thermocompression as a promising option for the fabrication of tailor-made, low-cost microfluidic devices featuring small channels for specific applications in the analytical chemistry field.

Additionally, 3D printing does not require additional costly equipment rendering this technology more accessible than LTCC or COC-based fabrication methods. In this way it is possible to make available to all laboratories of the world low-cost technologies to spurring innovation in the field of microfluidics [10–12].

The 3D printing techniques based on stereolithography (SLA) and digital light processing (DLP) used in this work are more accessible than other configurations such as multiple jet printing (MJP) [13,14].

2. Materials and Methods

3D printing was made with an Epax printer model X1 (Epax, Morrisville, North Carolina, U.S.A.), using 140 mm (5.5 inches) LCD SLA technology with 2K resolution (2560 x 1440 pixels) and 40W power compatible with 405 nm photosensitive resins. Resins used were ELEGOO ABS-Like Photopolymer Resin (ELEGOO, Shenzhen, China) in four tints: clear, red, black and green. A translucent resin supplied by ANYCUBIC (Shenzhen, China) was also used. The program Fusion 360 (Autodesk, San Francisco, California, U.S.A.) was employed to develop the 3D structures. The configuration and generation of the files fed to the 3D printer were produced with the program ChiTuBox Basic 1.9.4 (ChiTuBox, Shenzhen, China), for SLA/DLP/LCD printers. Data and dimensions were analyzed with OriginPro 2023B software (Northampton, Massachusetts, U.S.A.). Models were post-cured in a 405 nm curing box supplied by SUNLU (SUNLU, California, EE. UU.), featuring a rotating plate and a 60 W lamp.

All reagents used throughout this work were analytical grade. The stock copper solution for ICP (1000ppm), the disodium phosphate (Na_2HPO_4), the monosodium phosphate (NaH_2PO_4) and the nitric acid (HNO_3) were supplied by Sigma-Aldrich (Darmstadt, Germany). The 3-Hydroxy-4-nitroso-2,7-naphthalenedisulfonic acid disodium salt (NRS) was supplied by Fluka (Honeywell, North Carolina, U.S.A.). Working copper (II) solutions were prepared by successive dilutions from a 10-ppm stock standard copper (II) solution. A phosphate buffer solution (adjusted to pH 6.6), a 1.1 mM dissolution of the NRS reagent and a 0.01M HNO_3 solution were prepared using MilliQ water.

Transmittance was measured with a UV-Vis spectrophotometer series AM1706003 (Shanghai Metash Instruments, Shanghai, China). The microfluidic modules printed in resin were designed according with a lock & key configuration [15] [Versatile Lock and Key Assembly for Optical Measurements with Microfluidic Platforms and Cartridges. Oriol Ymbern, Miguel Berenguel-Alonso, Antonio Calvo-López, Sara Gómez-de Pedro, David Izquierdo and Julián Alonso-Chamarro, Anal. Chem. 2015, 87, 1503−1508]. DOI: 10.1021/ac504255t] featuring a 505 nm light emitting diode (Roithner Lasertechnik B5B-433-B505, Farnell, Spain) and a Hamamatsu S1337-66BR photodiode (Farnell, Spain).

NResearch three-way microvalves 161T031 (NResearch, Switzerland) were used for all fluid-handling operations including multicommutation, stock solutions preparation by automatic dilution, as well as sample, nitric acid cleaning solution and water intake. Fluids were impelled by an ISMATEC peristaltic pump ISM852A-115V60H (Cole-Parmer, Vernon Hills, Illinois, U.S.A.) connected to 1.2 mm Tygon (1Ismatec, Switzerland) and 0.8 mm i.d. polytetrafluorethylene (PTFE) (Tecnyflour, Spain) tubing.

The electronic control module was designed using the software EAGLE 9.3.1 (Autodesk, San Francisco, California, U.S.A.). The printed circuit of the module was designed using the software JLC (Shenzhen JLC Electronics Ltd., Shenzhen, China). The module was assembled and soldered by the authors. The main control element of the module is a programmable system on a chip, specifically

Preprints.org (www.preprints.org) | NOT PEER-REVIEWED | Posted: 24 December 2024 doi:10.20944/preprints202412.2045.v1

the integrated circuit PSoC 5 CY8C5868AXI-LP035 (Infineon, Neubiberg, Germany). Figure 1 shows the general diagram of the experimental setup used to test the microfluidic devices.

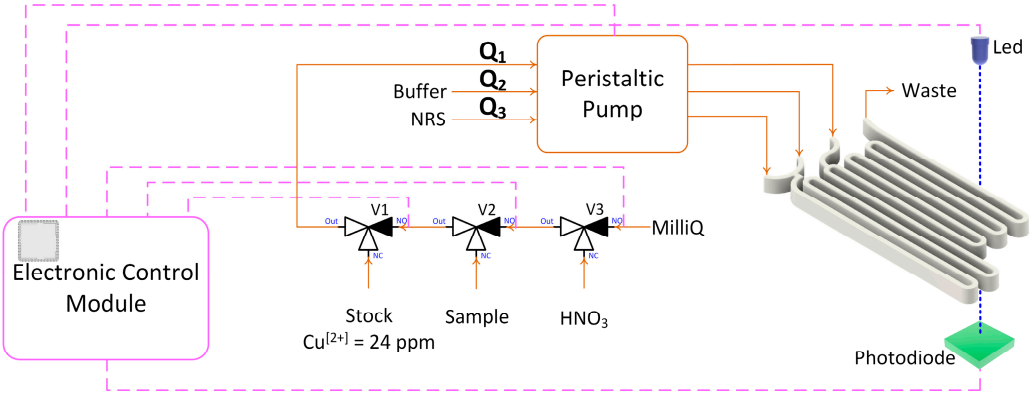

Figure 1. Copper Microanalyzer: Peristaltic pump; 3-way valves (V_1, V_2 y V_3); microfluidic platform; detector (LED 505nm and photodiode); Electronic control module and waste. --- Electronic connections between different modules.

Microfluidic platform fabrication method

To achieve high precision and a high quality in a 3D printer it is imperative to calibrate it appropriately. The patterns shown in figure 2 were used to ensure that the devices had the correct dimensions and to determine the optimal printing parameters, the thickness of the layers and the exposure times for each of the resins. [15,16].

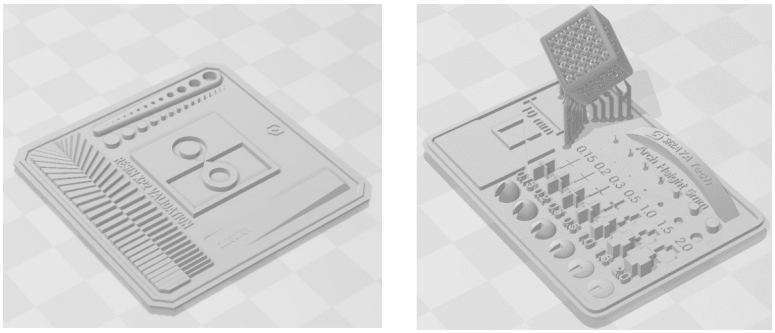

Figure 2. Patterns used for the calibration of the lamination parameters.

Figure 3 shows a simplified layout of the printing process using UV photosensitive resin and SLA LCD technology. From left to right, in stage (1) the initial layer is cured. The build platform dips into the pool of liquid resin to a distance from the bottom that equals the thickness of the next layer. This layer of uncured resin between the previously cured layer and the bottom of the resin tank, made of transparent fluorinated ethylene (FEP) is left exposed to the light from the curing lamp. The first few layers receive a longer exposure time to ensure a good adhesion to the build plate making sure that the increasing weight of the printed device does not detach IT from the build plate. In some printers the surface of the build plate is not smooth PRESENTING a rugged pattern that IT'S TRANSFERRED on the fixation layer. In stage (2) the build platform is raised leaving the next layer of resin to be cured between the build plate and the FEP bottom of the resin tank. In stage (3) this next layer is irradiated and cured, the 3D structure arises from the succession of curing STEPS and joining of the layers.

 doi:10.20944/preprints202412.2045.v1

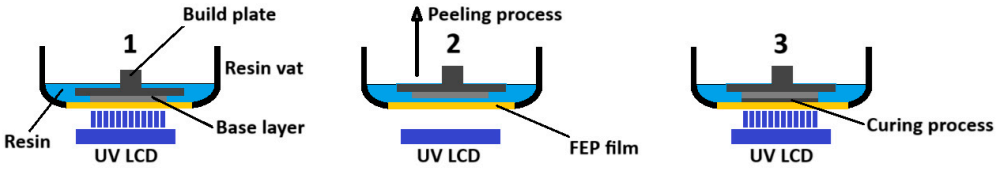

Figure 3. Simplified diagram of the 3D printing process using SLA LCD.

To build microfluidic devices with channels of 1mm x 1mm approximately, two fabrication methods were followed. The first method consisted of the construction of a monolithic microfluidic platform in a single block. During its manufacturing process, the definition of the embedded microchannels by selective irradiation of the layer where they are integrated poses the problem that the microchannels remain filled with uncured resin. To prevent the photocuring of the resin trapped in the microchannels, both in the layer of the microchannels and in the additional layers deposited to act as a cover, a minimum light exposure time was applied. Thus, the times for the two initial fixation layers were 40 seconds and 6 seconds for all the following layers. The thickness of each layer was 50 μm.For the second method a multilamination approach was followed. Two separate blocks were printed and then glued together to form the microfluidic device. The layer thickness was 50 μm and the exposure times were 50 sec for the two fixation layers and 8 sec for the rest of the layers. Key considerations for the design of the devices based on layers were as follows:

1. The full 3D design was made using computer aided design (CAD) software.
2. The two blocks (halves) forming the device were defined. In one of them there are the open microchannels that were printed. The open channels facilitate the removal of the uncured resin. The other block will be used to seal the microchannnels
3. The individual blocks can have a different thickness since they can have a different number of layers.
4. Both blocks are joined by multilamination using a photocurable resin.

Once printed, the block with the structured microchannels is cleaned with isopropyl alcohol to remove the uncured resin, which is filling the microchannels. Then the side of each block that contacted the build plate is polished to remove the rugged pattern transferred by the plate. Figure 4 shows the difference between a polished and a non-polished surface. The final assembly of the device was carried out by joining both blocks with a thin layer of photocurable polymer, deposited on one of the faces (layers) to be assembled. The joining of both blocks is achieved by irradiation with no pressure applied, as the adhesive force of the uncured resin holds both blocks together. Once aligned the Resin is Photocured for 60 s at 60 W.

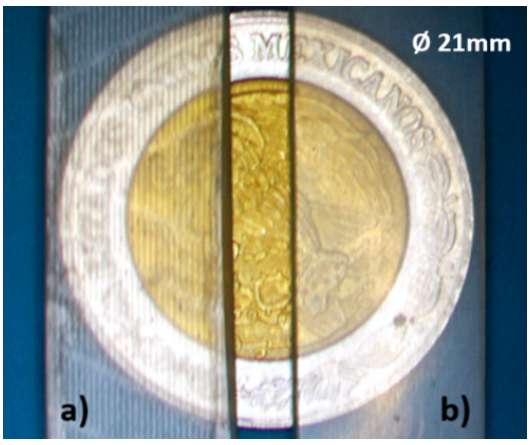

Figure 4. Final surface of the microluidic platform before (a) and after(b) it´s polishing.

 doi:10.20944/preprints202412.2045.v1

The layer of photocurable polymer used to join both halves of the 3D printed microfluidic structure was deposited using a steel spatula in accordance with the following procedure:

1. The spatula is loaded by dipping it no more than 1 mm perpendicular to the surface of the resin.
2. The spatula is withdrawn and left to drain the excess resin.
3. The block with the largest surface area is chosen. This is generally the one that acts as a lid closing the microchannels on the other block.
4. The spatula is dragged at approximately 45 degrees respective to the surface where the resin is applied, taking care to spread it uniformly.
5. Both BOCKS are aligned and joined without pressure to prevent the uncured resin from going into the microchannels.
6. The microfluidic device is irradiated on both faces to attain a uniform and hermetic sealing.

Figure 5 shows the pieces used to build a microfluidic module with approximately 0.8mm by 0.8mm channels, designed to be used in a system like that reported by Guevara [3]. Placing the channels as shown avoids possible obstruction by resin draining due to gravity. The final dimension of the device is 54mm by 44mm.

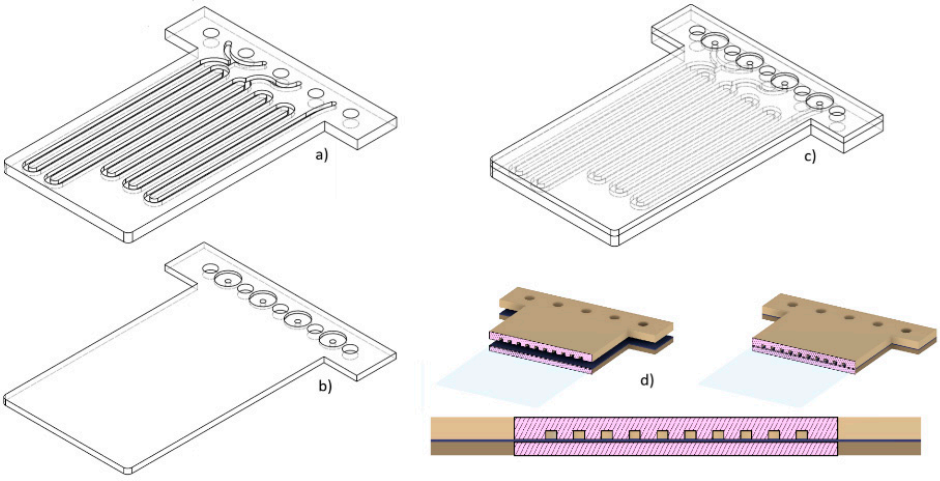

Figure 5. Example of a multilayered microfluidic design. The block a) incorporating the microchannels was bonded to the block b) to form the final microfluidic structure c). The uncured resin used for the bonding of both blocks was applied to the upper surface of block b). In d) a cross section of both sheets is shown during the alignment and bonding process.

3. Results

All 3D prints were made in an area approximately 54x44 mm. Single block prints were 3mm thick. The resin inside the channels was removed by injecting isopropyl alcohol using positive pressure via a syringe. To avoid photopolymerization of the resin inside the channels during printing, it was necessary to reduce the exposure time in all layers to the minimum recommended by the manufacturer. The reduction in exposure times cause insufficient adhesion between the layers, which, together with the viscosity of the uncured resin and the pressure applied to remove it from the channels, caused the separation of the layers and leaks in microstructures whose channels were greater than 50mm in length or microstructures featuring sharp turns intended to act as a mixer. Figure 6 shows some of the observed leaks.

 doi:10.20944/preprints202412.2045.v1

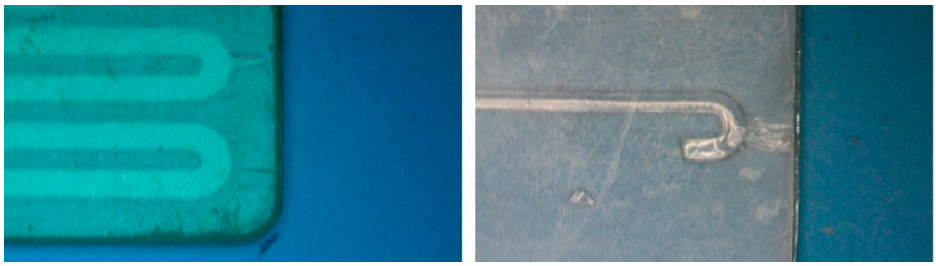

Figure 6. Layer separation and leakages in the microfluidic structure when pressure was applied to remove the uncured resin from the microchannels.

For the fabrication of devices by the multilamination based approach, the dimensions of the channel designed were initially 2x2mm, decreasing them in 0.2 mm steps until reaching channels of 0.2x0.2mm. The overall structure is composed of two blocks, one of them incorporating the opened microfluidic channels and the other one acting as a cover block. In Figure 7 the different channels without cover on one of the blocks can be seen. Channels with dimensions equal to or greater than 0.4mm presented good definition and repeatability.

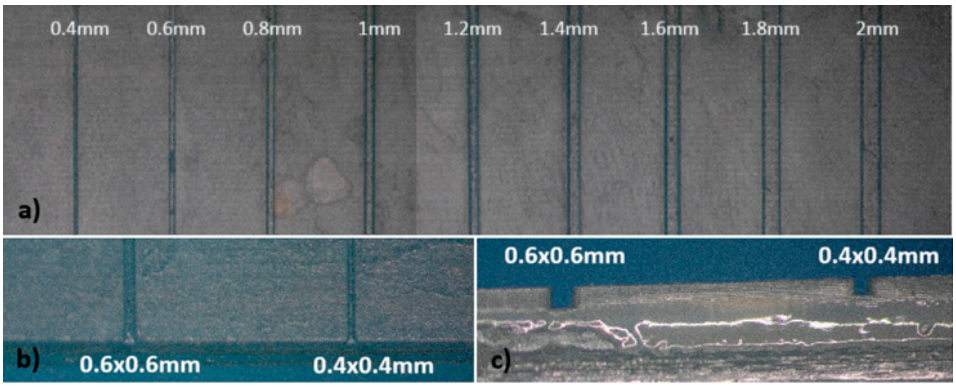

Figure 7. a) Zenithal view of the substrate incorporating straight open channels from 0.2 mm^2 to 2mm^2, b) Amplified zenithal and cross view of the channels 0.6x0.6 mm^2 and 0.4x 0.4 mm^2.

To evaluate the microfluidic structure produced using this method several micro-channels with identical dimensions were printed next to each other on the first block. Once both elements were joined, the resulting monolithic structure was cut and the cross-section area of each channel was measured at various points.

Figure 8 shows photographs of the cross sections of several printed and multilaminate monolithic structures obtained with different resins: a) ELEGOO green resin; b) ELEGOO transparent resin. In the amplified photograph shown in c) you can see that the joining of the two elements results in a single monolithic block where the interface between them is not visible.

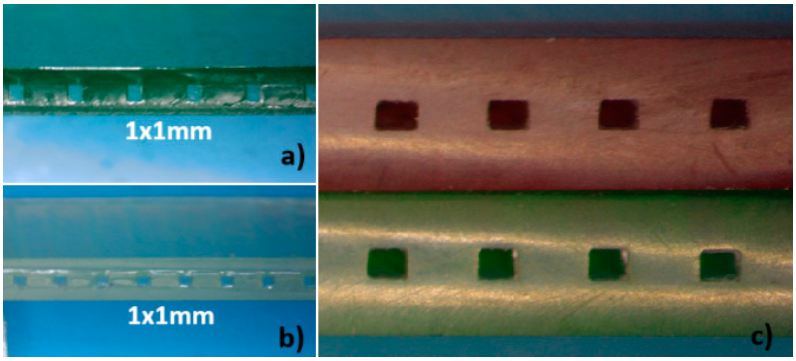

Figure 8. Channel cross sections view of the monolithic microfluidic structures. a) 1x1mm straight microchannel (ELEGOO green photocurable resin, b) 1x1mm straight microchannel (ELEGOO clear

 doi:10.20944/preprints202412.2045.v1

photocurable resin); c) Amplified view of the monolithic microfluidic block after the multilamination process.

It was noted that the resin used to join the two elements penetrated the microchannel causing a decrease in its height. The mean height reduction was 0.135 mm, with a standard deviation of 0.02 mm. The thickness of the sealing polymer layer after photocuring is no larger than 0.150mm. This reduction must be considered during the design process to achieve the desired channel sizes.

The microfluidic structures developed with this methodology were ready for use after curing the resin layer used to join the two elements.

The smallest channels constructed were 0.4x0.4 mm, regardless of the resin used, yielding leakage-free microfluidic platforms.

Figure 9 shows the design, distribution of masks and number of layers used for the manufacture of the two blocks of the device shown in Figure 5. A layer thickness of 50 μm was used, so the final design had a total thickness of 3.2mm. The microfluidic platform comprised three fluidic inlets, two confluence points, two meander-based mixers and one outlet.

Figure 9. Procedure followed during the 3D printing of the device shown in Figure 3. A) Experimental set-up. B) Design, distribution of masks and number of layers used for the fabrication of blocks 1 and 2.

 doi:10.20944/preprints202412.2045.v1

For analytical applications using optical measurements, it is important to integrate detection cells into microfluidic platforms whose optical path can be easily modified.

Considering that the detection cell is formed by a zone of the microfluidic channel, the fabrication methodology described above allows to easily increase the length of the optical path by varying the channel height. In this way, the dead volume of both the detection cell and the microfluidic system can be reduced. Both factors allow to limit sample dilution enhancing the sensitivity of the measurements. In Figure 10, different fabricated channels 1mm wide, with heights from 0.25 mm to 2mm, can be seen.

Modifying the height/width ratio of the microchannels to increase the optical path has other advantages. For instance, microchannels with ratios greater than 1 show greater resistance to deformation and are less susceptible to occlusion by the resin used as a sealant during the multilamination process.

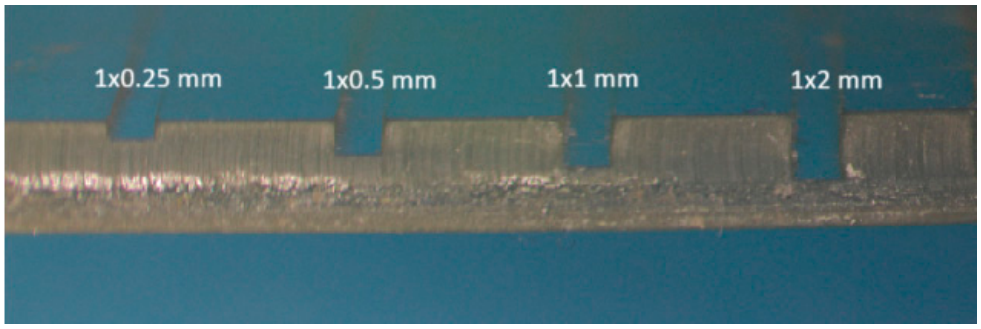

Figure 10. 3D printing layer with open channels of different height/width ratios and optical path lengths.

Figure 11 shows the transmittance spectrum obtained with 3mm-thick plates using the four ELEGOO resins (transparent, green, red, black) and the translucent ANYCUBIC resin.

The maximum transmittance was obtained at a wavelength of 505 nm using the green and transparent resins. In any case, the transmittance measured for all resins studied were below 30%. This fact seems to be related with the surface roughness of the first layer impressed in contact with the build plate.

Additional experiments performed with the transparent ELEGOO resin once the rough faces had been polished show a transmittance better than 60% for wavelengths higher than 425 nm. As can be seen, the polishing step is critical to enhance signal measured and then sensibility and detection limit of the analytical microsystem.

 doi:10.20944/preprints202412.2045.v1

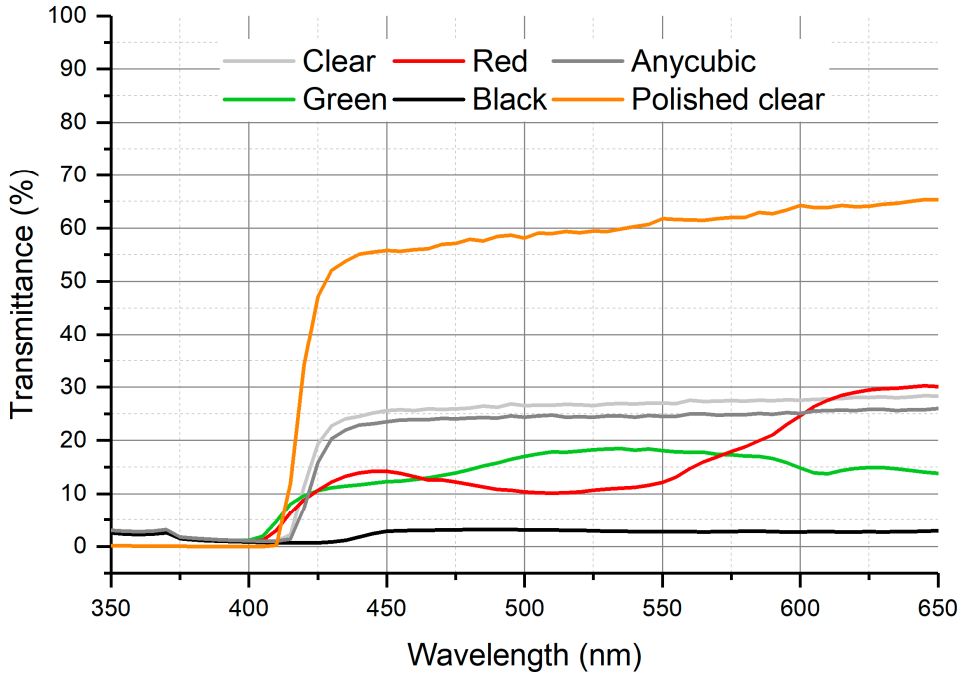

Figure 11. Transmittance spectrum using different resins.

To corroborate the usefulness of the developed 3D printed microfluidics using the described multilamination process, a microfluidic platform described in the Methods and Materials section (Figure 5 and Figure 9) was designed with a cross-sectional channel of 0.8x0.8mm for colorimetric determination of copper previously used by Guevara [3].

This microfluidic platform was incorporated to a multiconmutation flow system microanalyzer performing automatic sampling and autocalibration procedures which are like those described in [3].

Working at constant flow conditions, the sample volume injected depends on the actuation time of the 3-way valves used to select between sample/standard solution or carrier solution by commutation. To obtain robust microfluidic platforms not affected by slight changes in the experimental conditions, it was necessary to select a sample injection time that allowed the analytical signal to rise to its steady state. Figure 12 shows the results of the experiment performed at a fixed flow rate of 1.4 ml/min in each channel (Q1, Q2 y Q3) to determine the optimal injection time. The sample injection time selected was 120 s.

Finally, the multiconmutation approach allows to perform an automatic autocalibration procedure by “in-situ” generation of different standards solutions from a single concentrated stock solution.

 doi:10.20944/preprints202412.2045.v1

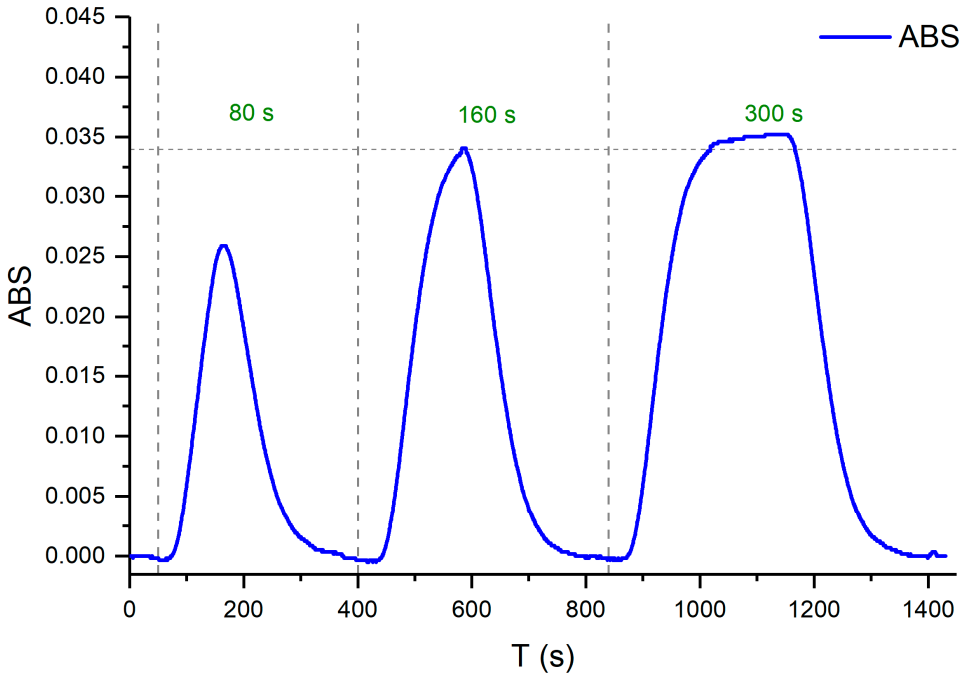

Figure 12. Analytical signal used to determine the injection time with a flow rate of 1.4ml/min.

Analytical features derived from the calibration plot obtained in the experimental conditions fixed after the optimization process shows a linear response in the range between 3 and 24 ppm of copper (II) with a correlation coefficient r2 >0.999. Figure 13 shows the analytical signals obtained during the autocalibration cycle featuring triplicate measurements.

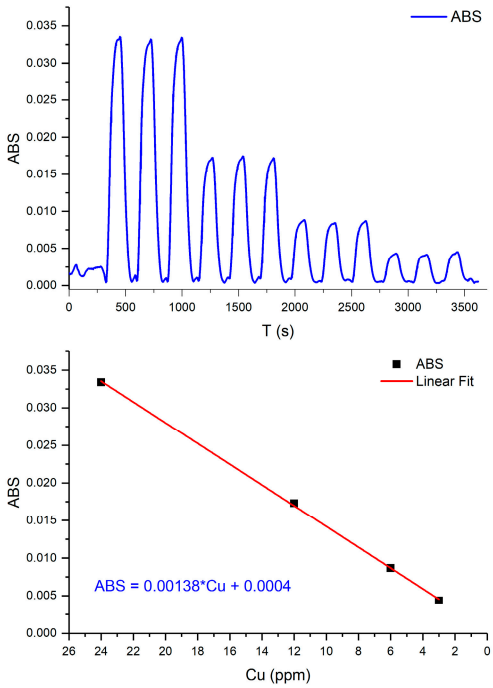

Figure 13. Analytical response of a calibration run and the resulting calibration curve.

To assess the reproducibility of the analytical signals provided by different micro-fluidic platforms operating at identical conditions, four of them were tested over a twelve-week period. All of them yielded similar results. The dimensions, polymeric resin, coloring, and structural integrity (no breakage or leakage) were maintained in all cases. The analytical results obtained with the devices fabricated with the 3D printing technology were comparable to those provided by microfluidic

 doi:10.20944/preprints202412.2045.v1

platforms made of COC using the multilamination approach. The main difference was the cost, as the micro-fluidic platforms described here were more affordable in terms of both materials and needed infrastructure.

4. Conclusions

The methodology described for the fabrication of fluidic systems using commercial low-cost UV 3D printers and resins allows for the rapid construction of microfluidic platforms with longer microchannels and more complex pathways. When designing the microchannels, an average reduction of 0.135 mm in the channel height should be considered. This reduction is caused by the resin deposited as an adhesive for bonding the two halves that constitute the microfluidic platform. The described method achieved better results than printing the entire platform in a single block, which is viable for short channels but presented issues of lack of rigidity and a high probability of breakage and leakage when attempting to remove the uncured resin from the microfluidic structures.

The microfluidic modules fabricated for copper detection were extensively tested, and it was observed that their dimensional integrity was maintained, and no leakages occurred. Their performance was identical to that of the platforms constructed with COC. The use of flat surfaces, along with the quality of the adhesion of the layers in the post-processing stage, opens the possibility of combining materials and technologies for future analytical flow applications.

The methodology described for the fabrication of fluidic systems using commercial low-cost UV 3D printers and fotoresins allows for the simple and rapid construction of microfluidic platforms with complex and longer microchannel pathways. The method proposed, based on multilamination approach, provides better results than the monolithic printing of the entire platform due to the difficulty to evacuate the uncured resin filling the microcanales.

A multiconmutation flow system microanalyzer for copper detection incorporating the microfluidic platforms fabricated were evaluated and optimized. It was observed that their operational performance and analytical features were identical to that of the platforms constructed with COC. The obtaining of flat surfaces with enhanced optical transmission obtained by polishing along with the quality of the adhesion of the layers in the post-processing stage, opens the possibility of combining materials and technologies for future analytical applications.

Author Contributions: Conceptualization, V.E.M.A., H.C.F.; methodology, V.E.M.A.; software, V.E.M.A, H.C.F.; validation, K.V.G.A., V.E.M.A. H.C.F and P.C.; formal analysis, V.E.M.A, H.C.F. and K.V.G.A.; writing—original draft, H.C.F., V.E.M.A. and K.V.G.A.; writing—review and editing, H.C.F., F.V.P., and J.A.-C.; supervision, F.V.P., and J.A.-C.; funding acquisition, F.V.P., and J.A.-C

Funding: The authors acknowledge Met-Mex Peñoles S.A. de C.V. and the Consejo Nacional de Humanidades, Ciencias y Tecnologías of Mexico (CONAHCYT) for financial support. The authors also would like to thank the financial support from the Spanish Ministry of Science and Innovation through the project PID2020-117216RB-I00 and Catalan government through the project 2021SGR00124.

Acknowledgments: The authors acknowledge to Tecnológico Nacional de México (TecNM), Instituto Tecnológico de la Laguna.

Conflicts of Interest: The authors declare no conflict of interest. The funders had no role in the design, collection, analyses, and interpretation of data of the study, nor in the writing of the manuscript or in the decision to publish the results.

References

1. G. Sanders y A. Manz, “Chip-based microsystems for genomic and proteomic analysis”, TrAC, vol. 19, núm. 6, pp. 364–378, 2000, doi: 10.1016/S0165-9936(00)00011.
2. N. Ibáñez-García, M. Baeza, M. Puyol, R. Gómez, M. Batlle, y J. Alonso-Chamarro, “Biparametric Potentiometric Analytical Microsystem Based on the Green Tape Technology”, Electroanalysis, vol. 22, núm. 20, pp. 2376–2382, 2010, doi: 10.1002/elan.201000133.

 doi:10.20944/preprints202412.2045.v1

3. K. V. Guevara Amatón y et al, "Microanalyser Prototype for On-Line Monitoring of Copper (II) Ion in Mining Industrial Processes", Sensors, vol. 19, núm. 3382, 2019, doi: 10.3390/s19153382.
4. S. Scott y Z. Ali, "Fabrication Methods for Microfluidic Devices: An Overview", Micromachines, vol. 12, núm. 3, p. 319, mar. 2021, doi: 10.3390/mi12030319.
5. Y.-J. Juang y Y.-J. Chiu, "Fabrication of Polymer Microfluidics: An Overview", Polymers, vol. 14, núm. 10, p. 2028, may 2022, doi: 10.3390/polym14102028.
6. P. Couceiro y J. Alonso-Chamarro, "Microfabrication of monolithic microfluidic platform using low temperature co-fire ceramics suitable fluorescence imaging", Anal. Chem., vol. 89, pp. 9147–9153, 2017, doi: 10.1021/acs.analchem.7b01889.
7. M. Berenguel-Alonso y et al, "Rapid prototyping of a cyclic olefin copolymer microfluidic device for automated oocyte culturing", SLAS Technol., vol. 22, núm. 5, pp. 507–517, 2017, doi: 10.1177/2472630316684625.
8. A. Calvo-Lopez, O. Ymbern, M. Puyol, J. M. Casalta, y J. Alonso-Chamarro, "Potentiometric analytical microsystem based on the integration of gas-difussion step for on-line ammonium determination in water recycling processes in manned space missions", Anal. Chim. Acta, vol. 87, pp. 26–32, 2015, doi: 10.1016/j.aca.2014.12.038.
9. J. Prada, C. Cordes, C. Harms, y W. Lang, "Design and manufacturing of a disposable, cyclo-olefin copolymer, microfluidic device for biosensor", Sensors, vol. 19, núm. 1178, 2019.
10. N. Bhattacharjee, A. Urrios, S. Kang, y A. Folch, "The upcoming 3D-printing revolution in microfluidics", Lab. Chip, vol. 16, pp. 1720–1742, 2016.
11. A. K. Au, W. Huynh, L. F. Horowitz, y A. Folch, "3D-printed microfluidics", Angew. Chem. Int. Ed., vol. 55, pp. 3862–3881, 2016.
12. B. C. Gross, J. L. Erkal, S. Y. Lockwood, C. Chen, y D. M. Spence, "Evaluation of 3D printing and its potential impact on biotechnology and the chemical sciences", 2014.
13. J. Taczała, W. Czepułkowska, B. Konieczny, J. Sokołowski, M. Kozakiewicz, y P. Szymor, "Comparison of 3D printing MJP and FDM technology in dentistry", Arch. Mater. Sci. Eng., vol. 101, pp. 32–40, 2020.
14. M. Pagac et al., "A review of vat photopolymerization technology: Materials, applications, challenges, and future trends of 3d printing", Polymers, vol. 13, núm. 598, 2021.
15. Versatile Lock and Key Assembly for Optical Measurements with Microfluidic Platforms and Cartridges. Oriol Ymbern, Miguel Berenguel-Alonso, Antonio Calvo-López, Sara Gómez-de Pedro, David Izquierdo and Julián Alonso-Chamarro, Anal. Chem. 2015, 87, 1503−1508. DOI: 10.1021/ac504255t]
16. Tech, S., "Siraya Tech Test Model". 2023.
17. Electronics, C., "Optimal Layer Exposure Time for Perfect Resin Prints - Tutorial Australia". 2023.
18. Anycubic, "Anycubic Photon Mono X - Google Drive". 2023.